

Simulated Free Field Measurements*

CHRISTOPHER J. STRUCK**, AES Member, AND STEVE F. TEMME***, AES Member

Brüel & Kjær, DK-2850 Nærum, Denmark

The development of time-selective techniques has enabled measurements of the free field response of a loudspeaker to be performed without the need for an anechoic chamber. The low-frequency resolution of both time-selective techniques and anechoic measurements is, however, limited by the size of the room. A technique is presented enabling measurements of the complex free field response of a loudspeaker to be performed, without an anechoic room, throughout the entire audio frequency range. It is shown that this technique can also be used for measurements of harmonic distortion.

0 INTRODUCTION

The purpose of this paper is to present a convenient and reliable method for obtaining the complete free field response of a loudspeaker in an ordinary room, making as few assumptions about the device under test as possible. Before attempting to obtain the free field response of a loudspeaker, it is useful to know what is meant by "free field" and "reverberant (or diffuse) field," as well as "far field" and "near field."

1 GLOSSARY OF IMPORTANT SYMBOLS

a	= radius of driver (or equivalent rigid, flat, circular piston)
b	= length of major semiaxis of ellipsoid
c	= speed of sound, = 344 m/s
d	= distance from source to measurement microphone (direct sound path)
d_0	= reference distance (e.g., 1 m)
d_R	= distance from source to first reflecting surface to microphone (path of first reflection)
F	= frequency range
f	= frequency
f_S	= transition frequency; near-field/far-field measurement
Δf	= frequency resolution (lower limiting frequency)
$H_{NF}(f)$	= near-field response of loudspeaker

$H_{FF}(f)$	= far-field response of loudspeaker
h	= length of minor semiaxis of ellipsoid
k	= wave number, (= $2\pi/\lambda$)
λ	= wavelength of sound
M	= largest linear dimension of source
N	= harmonic order
P_0	= reference electric power level (e.g., 1 W)
p_0	= reference sound pressure level (e.g., 20 μPa)
S_D	= effective surface area of driver
S_P	= effective surface area of port
T	= time range
Δt	= time resolution
τ	= time delay
τ_0	= delay in sound arrival corresponding to reference distance
x_0	= dB reference
Z_0	= nominal impedance of loudspeaker

2 FIELD DEFINITIONS

A free field describes idealized sound propagation with no reflections, that is, only the direct sound from a source can be observed. This occurs naturally in open outdoor spaces, high enough above the reflective surface of the earth. It can also be created artificially by constructing an anechoic room. In this case a large room is built using highly absorptive material on the walls, floor, and ceiling. The depth of the absorptive material is approximately equal to $1/4\lambda$ of the lowest frequency that can be effectively absorbed. In practical terms, this translates to a minimum room dimension of

$$h = 1.5\lambda \quad (1)$$

* Presented at the 93rd Convention of the Audio Engineering Society, San Francisco, CA, 1992 October 1-4; revised 1993 December 9.

** Currently with Charles M. Salter Associates, San Francisco, CA 94104, USA.

*** Now an independent consultant in Boston, MA, USA.

(see Fig. 1). Using the definition of the speed of sound,

$$c = f\lambda \tag{2}$$

this becomes

$$h = \frac{1.5c}{f} \tag{3}$$

For measurements down to $f = 20$ Hz, $h = 25.8$ m (without absorptive material). Another restriction is that the size of the device under test be small (approximately 1%) compared to the volume of open space available in the anechoic room [1]. The lowest usable frequency is therefore determined by the depth of the absorptive material and the smallest dimension of open space available, usually floor to ceiling height.

Often responses measured in smaller chambers ($h \approx 6$ m, $f \approx 100$ Hz) are plotted down to 20 Hz, perhaps due to the expense of constructing a large chamber. Fig. 2 clearly reveals the effect of an anechoic chamber on the measured response of a loudspeaker, particularly at low frequencies, even for an optimization of source and microphone positioning within the room. This is caused by the limited size of the anechoic chamber ($7.7 \times 6.5 \times 6.6$ m) and insufficient absorption of low-frequency reflections.

A reverberant field occurs when sound arrives from all directions with equal magnitude and probability. This can be approximated with a reverberation chamber, which is constructed with many irregular, highly reflective surfaces.

To be in the far field of a sound source, the wavelength of sound radiated should be large compared to the size of the source. This occurs in practice when the distance from the observer to the source is large compared to the size of the source. A so-called point source will radiate spherically ($4\pi sr$) into a free field in all directions if there are no reflections (see Fig. 3). Note that under these conditions the sound field is very well behaved and the sound pressure level changes by -6 dB for

every doubling of distance from the source, as shown in Fig. 4. This was verified in Fig. 2, where the level of the measured response decreases by 6 dB for each doubling of the microphone distance, empirically establishing that the microphone is in the far field of the source. For long, narrow line sources, the sound radiation will be cylindrical (see Fig. 5). In this case the sound pressure level will change by -3 dB for every doubling of the distance from the source. In practice, these conditions only exist over a limited frequency and distance range for a finite-size source and finite-size room.

When the distance to the source is small compared to the wavelength of sound, one is said to be in the near field of the source. This typically occurs at low frequencies, where the wavelength (and radius) of a spherical wave is so large that the sampled section of the wave is essentially a plane.

Therefore it can be said that the far field and the near field are determined by the *relative size of the source* compared to the frequency of the sound radiated. The free field and the diffuse field are functions of the *room or environment*.

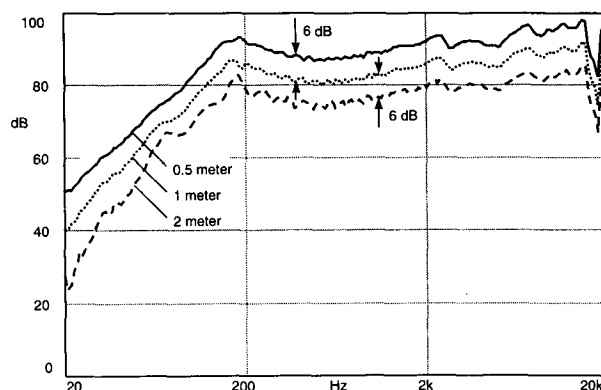


Fig. 2. Frequency response of a loudspeaker measured in an anechoic chamber for various microphone distances. Note 6-dB change in level for each doubling in distance. Ripple in response is due to insufficient absorption of reflections at low frequencies.

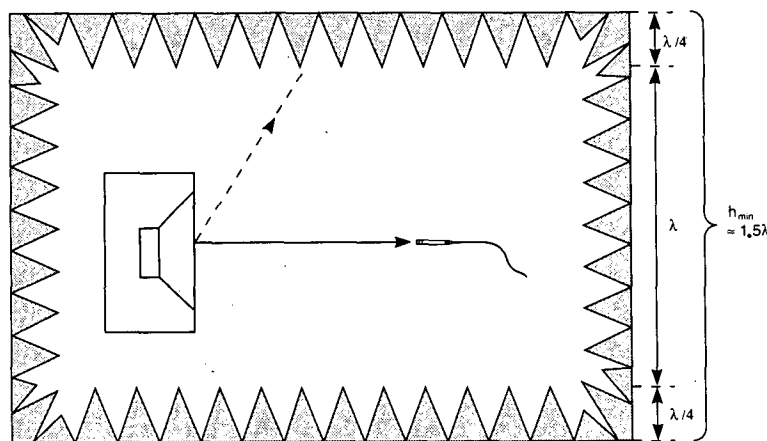


Fig. 1. The lower limiting frequency for anechoic measurements is determined by the depth of the absorptive material and the size of the room.

3 TIME-SELECTIVE TECHNIQUES

All time-selective techniques rely on the constant speed of sound in order to separate the desired direct sound component from reflections, which arrive at the measurement microphone delayed due to a longer traveled path [2]. Therefore differences between the various techniques are found only in terms of signal to noise ratio, measurement time, and frequency selectivity [1]. In practice the measurement time range T is limited in order to exclude unwanted reflections and noise. This can be done as part of the measurement or as post-processing. The uncertainty principle, in turn, determines the frequency resolution Δf of the measurement. Disregarding the actual shape of the time window for the moment, this is

$$\Delta f = \frac{1}{T} \tag{4}$$

The relation holds for *any* analysis or technique.

Using time-selective techniques, it is possible to obtain the free field response of a loudspeaker by measuring in an ordinary room. This is done by restricting the time range to prevent reflections from entering the measurement. Fortunately no special treatment of the walls, floor, or ceiling is necessary. The absorption influences the reverberation time, however, and consequently the total measurement time for impulse and gating techniques [2].

Fig. 6 shows a loudspeaker and a measurement microphone situated in an ordinary room. The distance traveled by the direct sound is d . From the loudspeaker to the nearest reflecting surface to the microphone, the sound travels a total distance of

$$d_R = d_{R1} + d_{R2} \tag{5}$$

The difference in path length between the direct sound and the first reflection determines the time available for

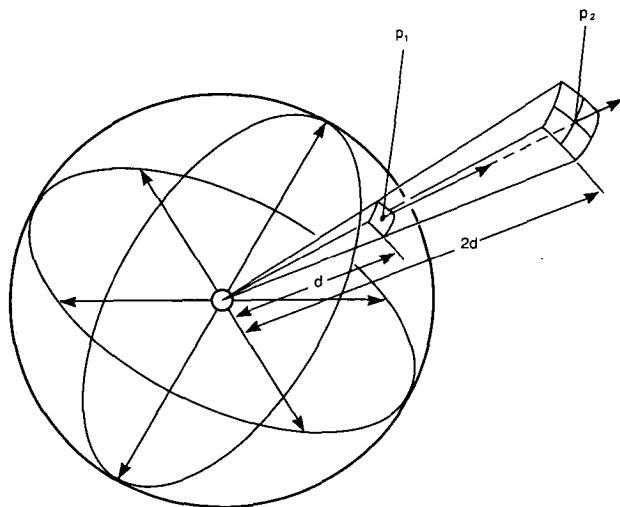


Fig. 3. Ideal point source radiating into free field. Sound pressure level decreases by 6 dB for every doubling of distance from source.

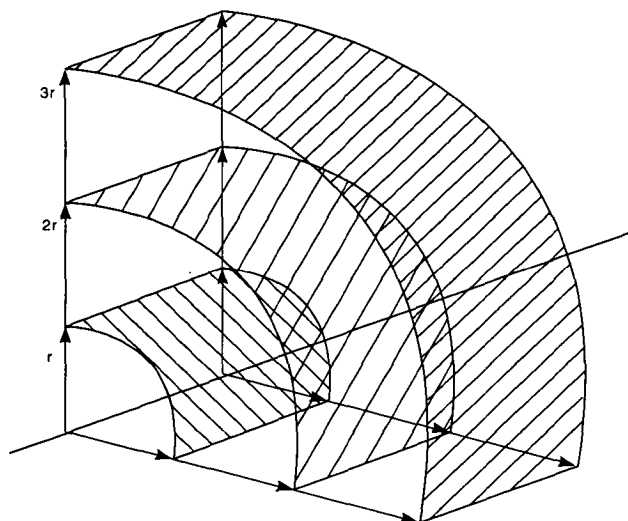


Fig. 5. Ideal line source radiating into free field. Sound pressure level decreases by 3 dB for every doubling of distance from source.

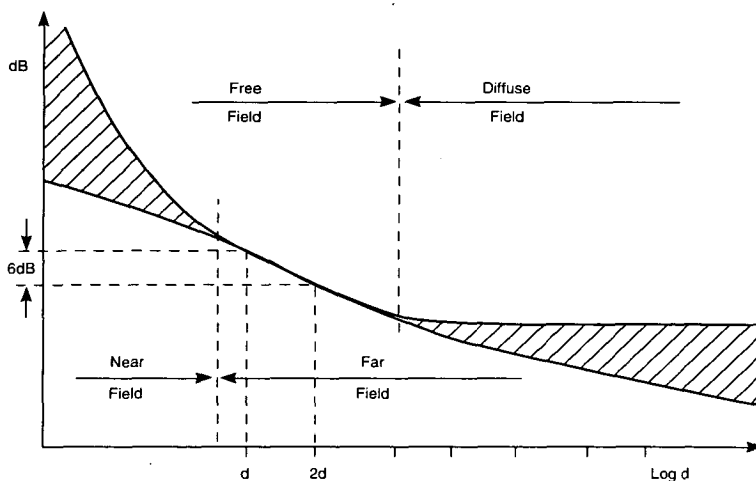


Fig. 4. Definition of sound fields for point source. Near and far fields are functions of the source; free and diffuse fields are functions of the environment.

a free field measurement,

$$T = \frac{d_R - d}{c} \tag{6}$$

where c is the speed of sound. This, in turn, determines the lower frequency limit for the measurement. From Eq. (4),

$$\Delta f = \frac{c}{d_R - d} \tag{7}$$

It is easily seen that the loudspeaker, measurement microphone, and nearest reflecting surface define an ellipsoid, with the loudspeaker and microphone at the focal points. The ellipsoid is a solid body of rotation, containing no reflective surfaces, about the major semiaxis which contains the microphone and loudspeaker focal points. Any surface touching the outer shell of the ellipsoid will cause a reflection to appear at the microphone that has traveled a distance d_R .

In general, the distance traveled by the first reflection is equal to the length of the ellipsoid along the major semiaxis,

$$\begin{aligned} d_R &= b \\ &= \sqrt{h^2 + d^2} \end{aligned} \tag{8}$$

For the typical case where

$$d_R = 2d \tag{9}$$

the height of the ellipsoid along the minor semiaxis h is found to be

$$\begin{aligned} h &= \sqrt{h_R^2 - d^2} \\ &= d\sqrt{3} \end{aligned} \tag{10}$$

usually the floor-to-ceiling height. The eccentricity of the ellipse ϵ is defined as the ratio of the distance between the focal points to the length of the ellipse along the major semiaxis,

$$\begin{aligned} \epsilon &= \frac{d}{b} \\ &= 0.5 \end{aligned} \tag{11}$$

The ratio of the length of the major semiaxis to the length of the minor semiaxis is

$$\frac{b}{h} \approx 1.15 \tag{12}$$

The problem of optimization then becomes that of placing the largest possible ellipsoid with eccentricity $\epsilon = 0.5$ within a given room. In an ordinary rectangular room this is usually done by centering the major semiaxis of the ellipsoid b along the longest horizontal room dimension L . If $L > 1.15h$, we obtain from Eq. (10)

$$\begin{aligned} d &= \frac{h}{\sqrt{3}} \\ &\approx 0.58h \end{aligned} \tag{13}$$

For $L < 1.15h$,

$$d = \frac{L}{2} \tag{14}$$

In general it is not worthwhile to carry the optimization too far, as will be seen in Section 4. It is useful, however, to keep a mental picture of the ellipsoid when arranging the test setup in the room in order to avoid the influence of disturbing objects that may cause reflections [2]. For this application the magnitude of the time response is

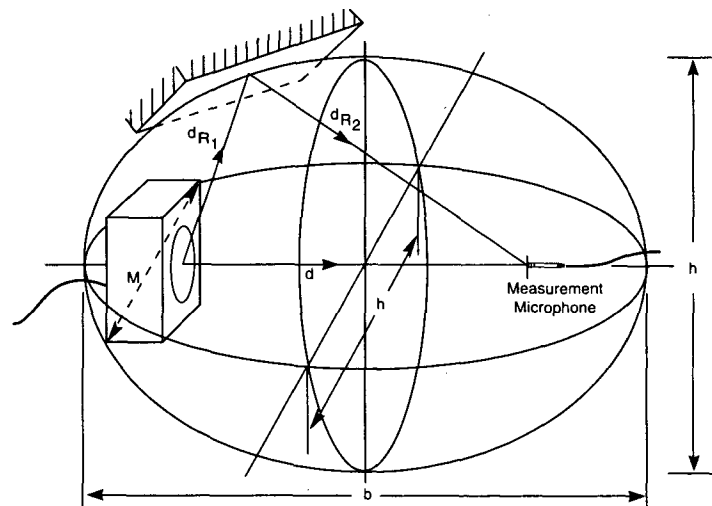


Fig. 6. Loudspeaker, measurement microphone, and nearest reflecting surface define an ellipsoid within which free field measurements can be performed using time-selective techniques.

useful for viewing the arrival of the direct-sound component, accurately fixing the measuring microphone distance, and determining the delay before the arrival of the first reflection.

For the response to be measured in the far field of the source, d should be at least 3 times the largest linear dimension of the source M ,

$$d > 3M. \quad (15)$$

Depending on the size of the source, this may be some distance other than 1 m (or other reference distance). Because simulated free field conditions have been obtained (that is, the sound field is well known), the measured response can easily be normalized to any desired reference (see Appendix 1). For measurements in the far field of the source, the distance d is then determined by the size of the device under test. In general, assuming Eq. (15) is fulfilled and substituting Eq. (8) into Eq. (7), we obtain

$$\Delta f = \frac{c}{\sqrt{h^2 - d^2} - d} \quad (16)$$

This expression is deliberately left unsimplified [using the assumptions of Eqs. (9), (10), (12), and (14)] in order to show the dependence of Δf on both room size and test object size if Eq. (15) is also fulfilled. Therefore the lowest measurable frequency using any time-selective technique is a function of the room size, where h is the smallest room dimension (usually floor to ceiling height), and the test object size, which determines the distance to the measurement microphone d according to Eq. (15).

Whenever attempting to visualize this problem mentally, it is useful to think of a "small box (the loudspeaker) inside a large box (the room)." When the ratio between room size and loudspeaker size is large, it will be relatively easy to perform simulated free field measurements over a wide frequency range F . As the ratio decreases (that is, the room size is decreased or the loudspeaker size increased), it will become increasingly

difficult to perform free field measurements.

In contrast to gating, or to the time-delay spectrometry technique, where the time window is determined by the use of a tracking filter [3], it is advantageous to apply the time window as a postprocessing operation [4]. This is done in order to have a more well-defined time window and to obtain the optimum frequency resolution. It also allows the entire measurement, including reflections, to be viewed in the time domain before applying the window. This implies an inherently linear, constant bandwidth data format for the far-field measurement for use of the forward and inverse Fourier transforms. Reflections are removed from the far-field measurement by multiplying the measured response (in the time domain) by a window function. Consequently the frequency response is convoluted with the Fourier transform of this window. Empirically, through much trial and error, we have found that the optimum time selectivity and the minimum resulting frequency-domain spreading are obtained by the use of a variable-width rectangular time window with leading and trailing Hanning (\cos^2) tapers of 10% of the rectangular width (see Fig. 7). With respect to worst-case frequency resolution, the effective time range T is determined by the width of the rectangular portion of the time window. It will be seen in Section 4 that the actual shape of the time window becomes less critical if the low-frequency response of the system can be obtained by another method.

As mentioned previously, the choice of excitation signal and test method should be based on speed, its effect on the test object, selectivity in both time and frequency, and the maximum available signal-to-noise ratio. In addition, it should be possible to specify the input power to the device under test accurately, unless the system is known to be perfectly linear. Transducers, and loudspeakers in particular, do not normally fall into the category of perfectly linear systems, particularly not over a wide dynamic range. The sine wave has a low crest factor and its power can be determined easily and precisely.

Sinusoidal excitation also enables ideal frequency selectivity, offering the possibility for harmonic measure-

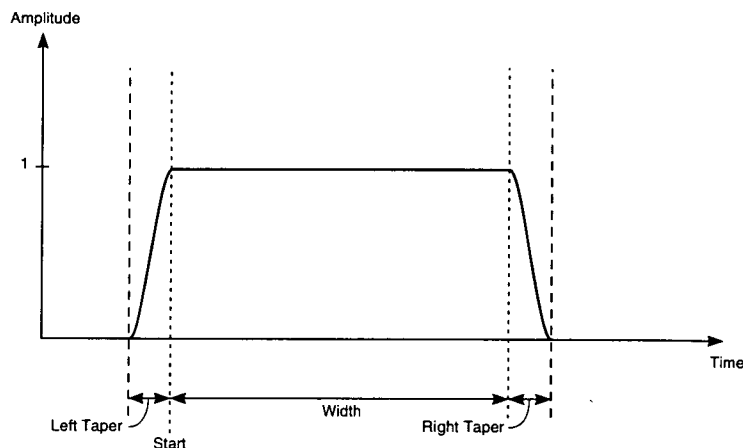


Fig. 7. Effect of reflections can be removed from far-field measurement by multiplying measured time response by a time window. This window is rectangular with Hanning tapers to reduce frequency-domain spreading.

ments. The time required for the far-field measurement should be determined entirely by background noise. In an ordinary room this should be no more than about 1 s [5]. A short measurement time will also minimize time variance, such as effects due to heating. It should be kept in mind, however, that an improvement of 3 dB in the signal-to-noise ratio can be gained for every successive doubling of the effective measurement time [3], [6].

4 NEAR-FIELD MEASUREMENTS

The low-frequency response of a loudspeaker can be obtained using the near-field technique [7]. This is done by simply moving the microphone very close to the low-frequency driver(s) in the loudspeaker system (see Fig. 8). This, of course, assumes that there is little or no passive radiation from the walls of the enclosure, that is, the structure is essentially rigid. To avoid measurement errors, the measurement microphone should be as close as possible to the driver under test.

A microphone distance of

$$d < 0.11a \tag{17}$$

results in measurement errors of less than 1 dB. The

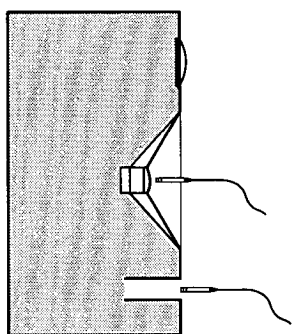


Fig. 8. Low-frequency measurements can be performed by placing microphone in near field of loudspeaker. Microphone should be placed as near as possible to center of diaphragm or port opening.

microphone should be placed as near to the center of the diaphragm as possible [7]. This technique physically eliminates reflections and noise. The near-field measurements can be carried out entirely in the frequency domain. The theoretical upper frequency limit for performing near-field measurements on a driver mounted in an infinite baffle is given by

$$ka = 1 \tag{18}$$

where k is the wave number. Substituting Eq. (2) into Eq. (18) becomes

$$f_{ka=1} = \frac{c}{2\pi a} \tag{19}$$

or

$$f_{ka=1} = \frac{58.749}{a} \tag{20}$$

for driver radius a in meters. For convenience, this can be rewritten as

$$f_{ka=1} \leq \frac{10\,949.86}{2a} \tag{21}$$

in terms of the driver diameter $2a$ in centimeters. Fig. 9 shows the upper limiting frequency for near-field measurements of drivers mounted in an infinite baffle versus driver diameter in centimeters. For driver diameters specified in inches, this becomes

$$f_{ka=1} \leq \frac{4310.97}{2a} \tag{22}$$

For closed or ported loudspeaker systems, this limit will be lower (see Section 5).

For ported loudspeakers or enclosures containing multiple drivers, additional near-field measurements of the

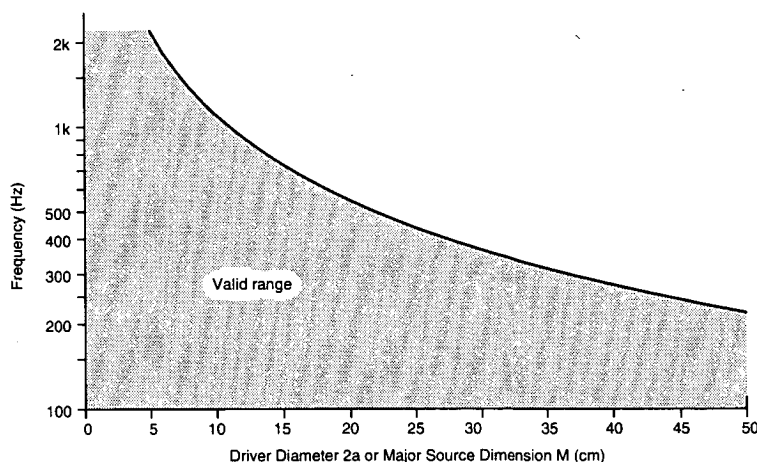


Fig. 9. Highest frequency at which near-field measurements can be performed is determined by size of driver when mounted in infinite baffle or largest dimension of enclosure. Upper frequency limits are shown versus driver diameter $2a$ or major source dimension M .

individual sources are required. The complete near-field response is found by first scaling the measurement of the port(s) and then taking the complex sum of all measurements [7] (see Appendix 2).

Because the microphone is so close to the driver (or port), the measured sensitivity appears considerably higher than an equivalent far-field measurement. For a loudspeaker system radiating into a 4π space, the far-field sensitivity can be calculated from

$$H_{FF}(f) = \frac{H_{NF}(f)a}{4d} \quad (23a)$$

or

$$H_{FF}(f) = H_{NF}(f) - 20 \log_{10} \frac{4d}{a} \quad [\text{dB}] \quad (23b)$$

where $H_{NF}(f)$ is the measured near-field response and $H_{FF}(f)$ is the far-field response at a microphone distance d for a driver of a radius a . For ported loudspeakers the radius a is taken as the radius of the driver. For a driver mounted in an infinite baffle, radiating into a 2π space, the far-field sensitivity can be calculated as

$$H_{FF}(f) = \frac{H_{NF}(f)a}{2d} \quad (24a)$$

or

$$H_{FF}(f) = H_{NF}(f) - 20 \log_{10} \frac{2d}{a} \quad [\text{dB}] \quad (24b)$$

This means that at low frequencies, where the loudspeaker behaves like a rigid piston, the measured near-field response is directly proportional to the far-field response and is independent of the environment into which the loudspeaker radiates [7], [8]. Alternatively, the level offset can be determined directly by comparison to a far-field measurement in the "overlap" frequency range,

$$\Delta f \leq f \leq f_{ka=1} \quad (25)$$

where both the near-field and the far-field measurements should be valid (see Fig. 10). The upper frequency limit for the overlap range is explained in Section 6. As it is usually not possible to reduce the size of the loudspeaker once it is created, it is necessary to perform the far-field measurements in a room of sufficient size so that an overlap frequency range exists. Combining the two methods of determining the sensitivity offset and solving Eq. (23) for the radius a , yields

$$a = \frac{2dH_{FF}(f)}{H_{NF}(f)} \quad (26)$$

for a frequency f in the overlap range, when $H_{NF}(f)$ and $H_{FF}(f)$ are measured independently, for a driver mounted in a baffle. For individual drivers, this interesting result provides an empirical method for determining the effective radius a and subsequently the effective radiating surface area of the driver S_D ($S_D = \pi a^2$). This parameter is critical in the determination of the Theile–Small parameters.

For frequencies above $f_{ka=1}$ most drivers no longer behave like rigid pistons (that is, modal behavior or "cone breakup") and the relationship between near-field and far-field response becomes complex. The frequency range for the near-field measurement should therefore be chosen to an upper frequency no greater than $f_{ka=1}$. The lower frequency should be less than or equal to 20 Hz (lower for large-diameter or extended-range woofers) in order to include the low-frequency rolloff of the system. This is important for examining the time-domain behavior of the system.

Near-field measurements are entirely independent of the measurement technique and offer the optimum measurement signal-to-noise ratio due to the proximity of the microphone to the sound source. This provides a high rejection of both correlated noise (that is, reflections) and uncorrelated random background noise. Using stepped sine excitation, tests can be performed at discrete frequencies in a logarithmic (ISO preferred) frequency format, typically 1/12 octave (ISO R40) or 1/24

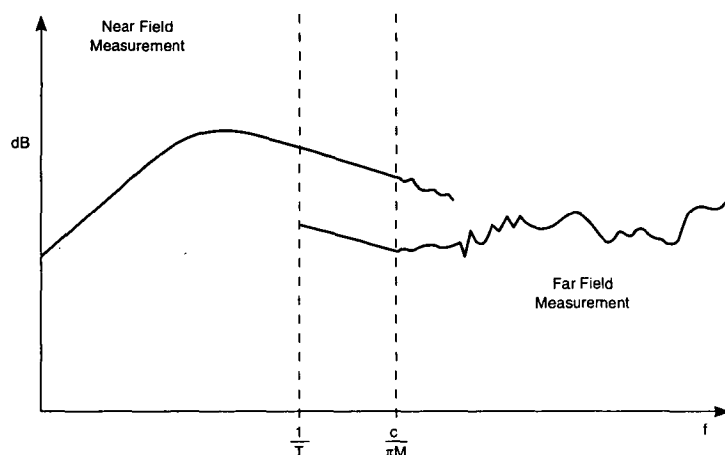


Fig. 10. For a sufficiently large room, a frequency range exists where both near- and far-field measurements are valid.

octave (ISO R80). This optimizes low-frequency resolution and test time and enables measurements of harmonic distortion to be performed [6].

5 FULL-RANGE RESPONSE MEASUREMENTS

If a full audio range response (typically 20 Hz to 20 kHz) is desired, the measurement can be performed in two passes. The first measurement is performed in the far field using a calibrated microphone. The microphone can then be repositioned into the near field to measure the low-frequency response. Assuming an overlap frequency range exists, a transition frequency f_s within this range can be selected at which to join these measurements. With the exception of the room size, no other assumptions are made. Postprocessing is then performed to account for the time delay to the far-field microphone, for the application of a time window to the far-field measurement to isolate the direct-sound component, and to account for the sensitivity offset between the far-field and near-field measurements. All block arithmetic operations should be complex so that other functions such as phase, group delay, and the time response are available for the final, full frequency range response data.

To test the application of this method, measurements were performed on a small (180 by 110 by 110 mm) two-way closed-box loudspeaker, with an 85-mm-diameter woofer using a Brüel & Kjær Type 2012 audio analyzer and a calibrated Brüel & Kjær Type 4133 free field microphone. The inherent phase inversion of the measurement microphone is corrected during the postprocessing. The output of the measurement system was calibrated to account for the gain and frequency response of the power amplifier used to drive the loudspeaker

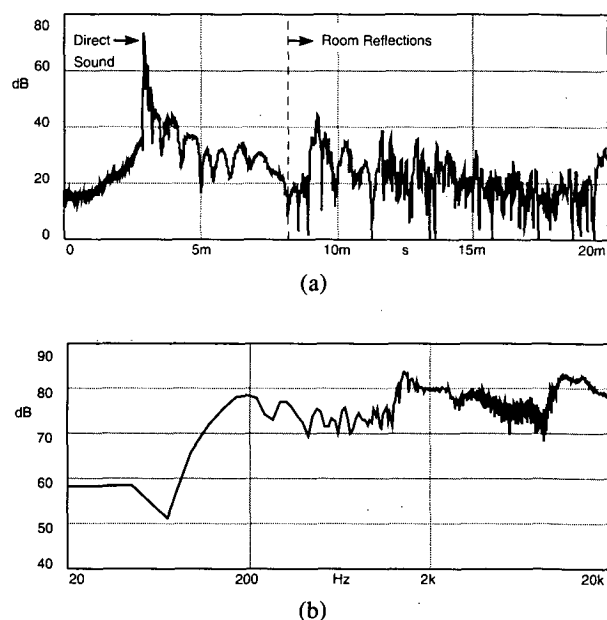


Fig. 11. (a) Magnitude of time response shows arrival of direct sound at measurement microphone followed by arrival of reflections. Effect of reflections appears as ripple in frequency response (b).

under test. This enabled direct measurement of the system response at the input and output terminals of the device under test. All postprocessing was carried out directly in the analyzer. In addition to the graphs shown here, the measurement results are available in ASCII format for further processing (such as polar response, directivity, and statistics).

First a measurement of the loudspeaker response in the far field is performed. The result is shown in Fig. 11, including the effect of room reflections. The time-response magnitude clearly shows the arrival of the direct sound as well as the delay before the arrival of reflections. The delay before the arrival of reflections determines the time range T available for a time-selective measurement. If the time range is insufficient, the microphone-loudspeaker setup must be repositioned or the measurements may need to be performed in a larger room. Reflections are convoluted with the response of the loudspeaker in the frequency domain, resulting in a "ragged" frequency response.

The peak in the time-response magnitude indicates the delay in sound propagation τ for the arrival of the direct sound at the microphone, and consequently the distance d to the microphone position (typically the tweeter arrival). A time shift can be applied to the far-field measurement to compensate for this delay, which is not an actual part of the loudspeaker response (see Fig. 12). This allows the final phase response to be displayed without "wrapping." It is followed by the application of the time window to the far-field measurement (see Fig. 13). The resulting frequency response appears "smoothed," due to the removal of time-domain reflections which cause frequency-domain ripple.

The microphone is then repositioned in the near field of the woofer, and the low-frequency response is measured. This appears with a higher sensitivity than the far-field measurement (see Fig. 14). The cursor can be

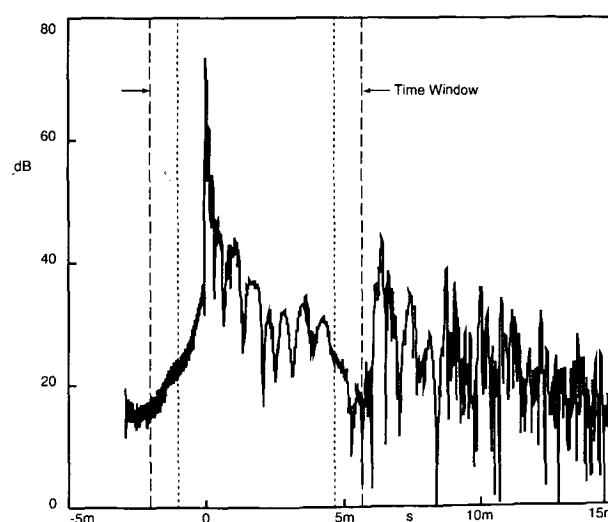


Fig. 12. A time shift is applied to measured response to account for delay to measurement microphone. This is followed by application of a time window to isolate the direct-sound component. Inner lines indicate rectangular portion of window ($T = 5.67$ ms); outer lines indicate leading and trailing Hanning tapers.

used to read the offset between the measurements to match the sensitivity of the high-frequency measurement. The magnitude of the offset can also be calculated according to Eq. (24). After rescaling the magnitude of the near-field measurement, an overlap region should be clearly visible. A transition frequency f_s can then be selected within this region.

In order to avoid a discontinuity in the phase response, both near-field and far-field measurements must be referred to the same acoustic reference plane. This is accomplished by applying a time shift to remove the appropriate delay from each measurement. The reference plane is established after time shifting the far-field measurement as previously mentioned by τ . If the intrinsic delay in the near-field measurement is τ_{NF} , then the delay to be removed from this measure in order to align it to the already compensated far-field measurement is τ_x (see Fig. 15). Noting that delay is the derivative of phase

with respect to frequency, this delay can be found by examining the phase difference $\Delta\phi$ (see Fig. 14) between the measured near-field phase and the compensated far-field phase at f_s . For "unwrapped" phase functions the delay compensation to be applied to the near-field measurement can be calculated as

$$\tau_x = -\frac{1}{360} \cdot \frac{\phi_{NF}(f_s) - \phi_{FF}(f_s)}{f_s} \quad (27)$$

for phase measured in degrees (see Fig. 16). The applied time-shift compensation has the opposite sign of the propagation delay to the microphone.

The near-field measurement is shown along with the far-field measurement in Fig. 16, after the application of Eq. (24) and after delay compensation. Note the alignment of the phase responses and the overlap range in the magnitude responses.

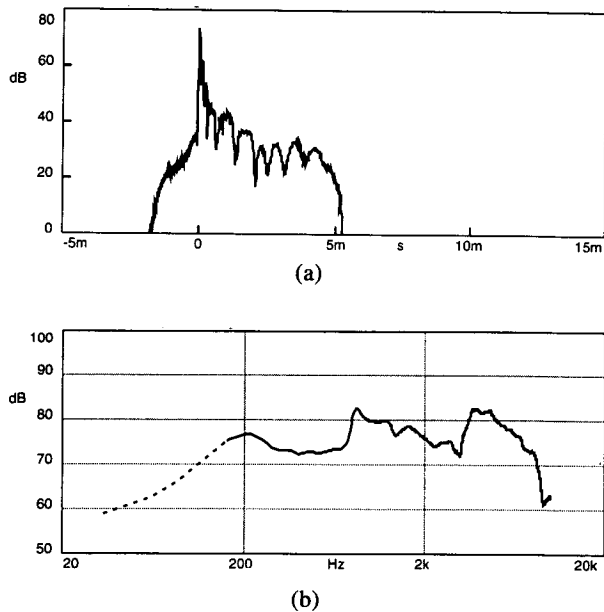


Fig. 13. (a) Time response (re 1 Pa/V) after application of time window. (b) Resulting frequency response (re 20 μ Pa/V), valid to $\Delta f = 1/T$ (176 Hz).

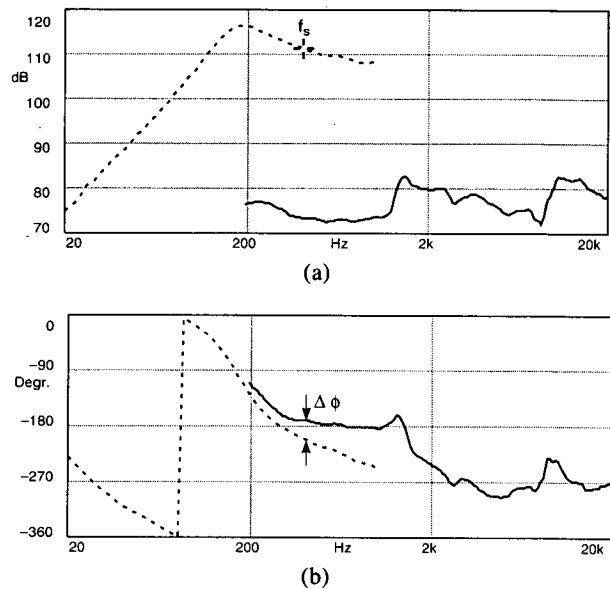


Fig. 14. Near-field measurement before magnitude and delay compensation. Low-frequency measurement shows higher apparent sensitivity compared to far-field measurement due to decreased distance from microphone. (a) Magnitude. (b) Phase.

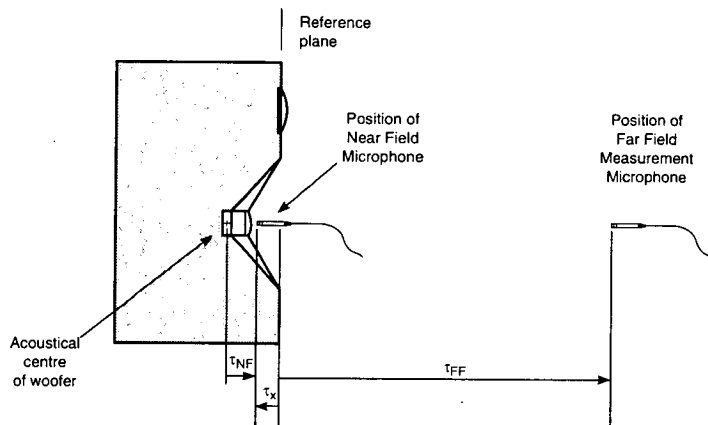


Fig. 15. Delay compensation applied to both near-field and far-field measurements in order to refer both to same acoustic reference plane.

In order to preserve the low-frequency resolution and to avoid a discontinuity in frequency resolution between the upper and lower frequency ranges at f_s , the linear (FFT) far-field data are converted to a logarithmic (constant-percent bandwidth) format equivalent to the ISO R80 format of the near-field measurement. This is a straight-line interpolation algorithm on a decibel versus logarithmic frequency axis. The linear data are 1600 points, from 1 Hz to 40 kHz, so the response should be more than adequately sampled for an accurate conversion in the frequency range where the windowed far-field data are valid. This has the added advantage of showing the response in the frequency domain in an optimum format, as it is universally accepted as standard industry practice to show the frequency response in decibels, on a logarithmic frequency scale, preferably with the IEC 263 axis ratio (25 or 50 dB per decade). A linear data set in the frequency domain tends to concentrate resolution at the higher frequencies on a logarithmic frequency axis. An additional benefit is that the final response contains the ISO preferred frequencies, so it is a simple matter to obtain the necessary values for the calculation of sensitivity, directivity, and so on.

Afterward rectangular frequency windows are applied to both measurements. The near-field low-frequency measurement is windowed to eliminate data at frequencies above f_s . The far-field measurement is windowed to exclude data at frequencies below f_s . Assuming $f_s > 1/T$, this also eliminates invalid data remaining after the application of the time window. Now the two responses no longer overlap. The final process is to add the two responses together to obtain a single, continuous complex data set. The last step is to divide out the complex response of the power amplifier used to drive the loudspeaker. The magnitude of the resulting frequency re-

sponse for the complete system, shown from 20 Hz to 20 kHz, appears in Fig. 17. The phase and the group delay are shown in Fig. 18.

Because the data are complex, the final response can be reconverted to a linear format (without the effect of reflections) before applying an inverse Fourier transform to recalculate the time-domain response from the full-range frequency response. In this way the measured data can be displayed optimally in both the frequency and the time domains. Extending the measurement frequency range F to 40 kHz normally eliminates the need for any windowing of the frequency response prior to calculation of the time response. Most loudspeaker systems designed for the normal audio range will be sufficiently rolled off, or "self-windowed," at both the upper and the lower ends of a 1-Hz to 40-kHz frequency spectrum. This subsequently eliminates artifacts caused by such windowing. The resulting time resolution Δt given by

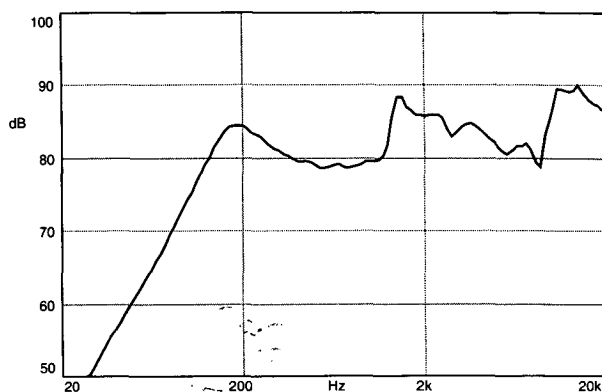
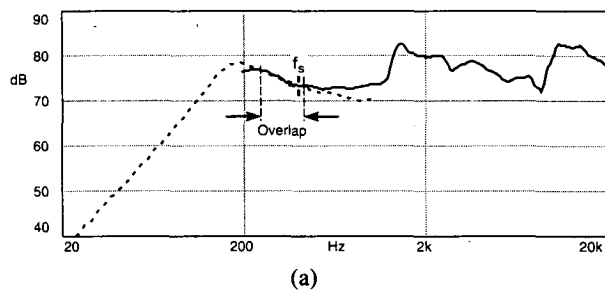
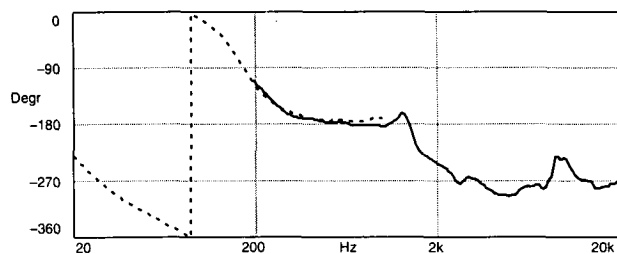


Fig. 17. Resulting on-axis frequency response, 20 Hz to 20 kHz, ISO R80 format (1/24 octaves), dB re 20 μ Pa/2.0 V at 1 m (1 W into 4 Ω), $f_s = 400$ Hz (two-way, 4- Ω , closed-box loudspeaker, grille off).

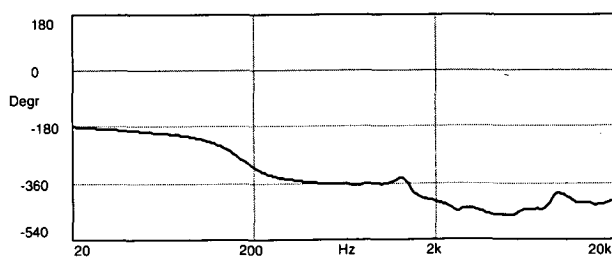


(a)

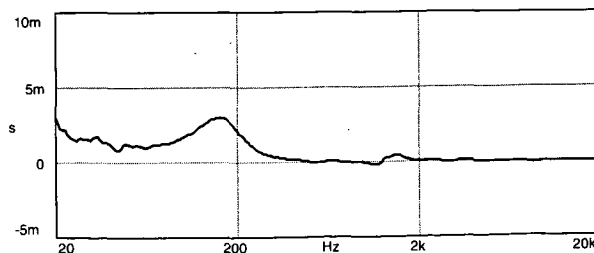


(b)

Fig. 16. Near-field response after application of level offset and delay compensation. Note overlap range in magnitude response where both measurements yield same result. Cursor indicates selected transition frequency. (a) Magnitude. (b) Phase.



(a)



(b)

Fig. 18. (a) Phase and (b) group delay for same two-way closed-box loudspeaker. Note that resulting data set is complex.

the uncertainty principle is

$$\Delta t = \frac{1}{F} \tag{28}$$

For an "extended-range" loudspeaker, with a frequency response that has not rolled off sufficiently at 40 kHz, a frequency window with a right-Hanning taper from 20 kHz to 40 kHz can be applied before calculation of the time response. This has the advantage of not affecting the frequency response in the audio bandwidth, and especially not affecting the response at low frequencies, and it is an improvement over the "half-Hann" window recommended in [9]. The magnitude of the time response is seen in Fig. 19. The real part of the time response (traditional impulse response) can also be displayed (see Fig. 20).

Software can be used to automate the entire process

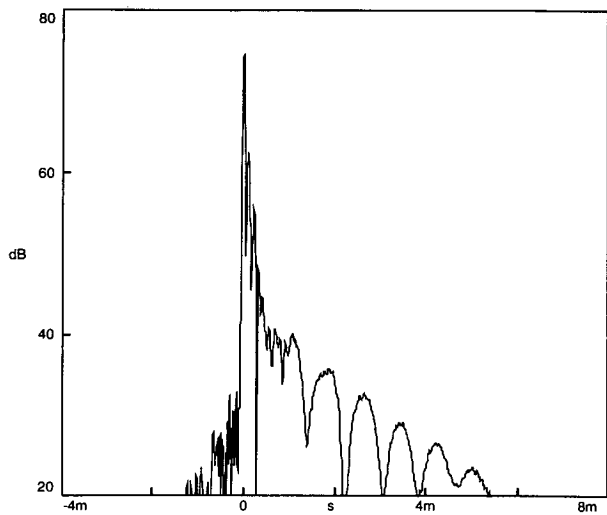


Fig. 19. Time response (magnitude) of system can be calculated from full-range frequency response by inverse FFT (right-Hanning taper, 20 kHz to 40 kHz, applied to frequency response before calculation).

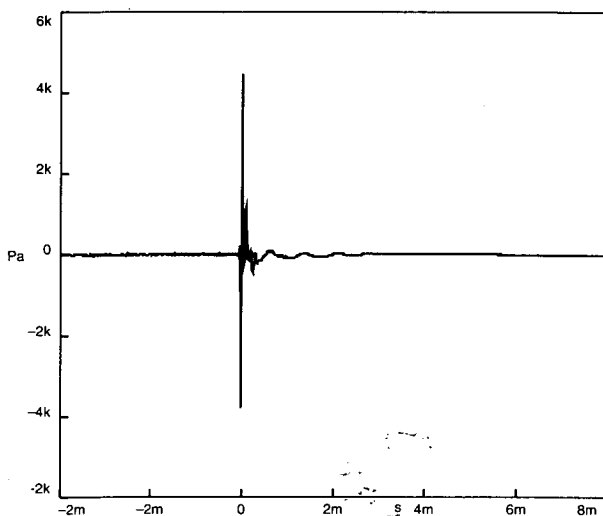
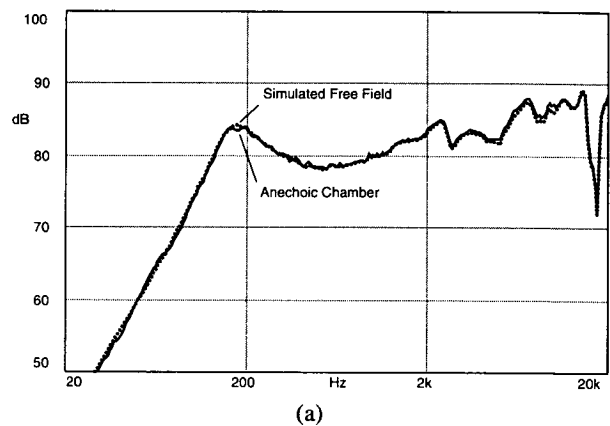


Fig. 20. Real part of time response (impulse response).

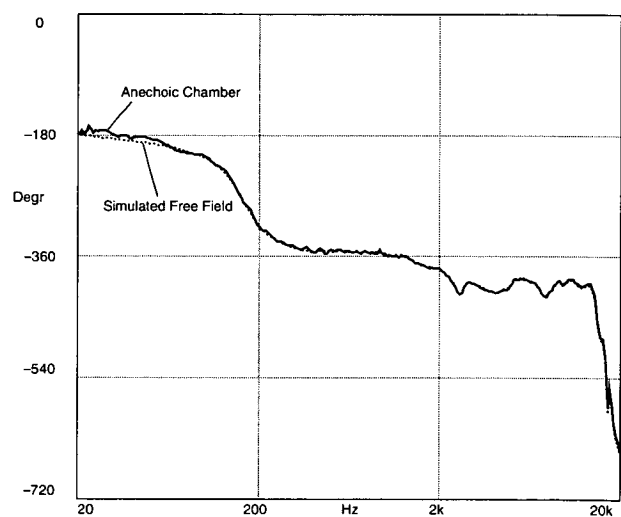
(except for moving the microphone for the near-field measurement), including guidance in performing both the measurements and the postprocessing as well as documentation of the results.

Fig. 21 compares the response of a similar loudspeaker measured in an ordinary room using this technique to the response of the same loudspeaker measured using traditional techniques (that is, not time selective) in an anechoic chamber. Differences at low frequencies are due to previously mentioned errors introduced by the size of the anechoic chamber (7.7 by 6.5 by 6.6 m), according to Eq. (3).

To test the technique further, a ported loudspeaker (39 by 23 by 22 cm) was also measured. Fig. 22 shows the individual measurements of the driver and the port. The measurement of the port is first scaled by the square root of the ratio of the port area to the effective radiating surface area of the driver (see Appendix 2). This scaled response is then summed (complex summation) with the near-field response of the driver. The complete near-field response of the ported loudspeaker is shown in Fig. 23. The resulting simulated free field response of the



(a)



(b)

Fig. 21. (a) Simulated free field technique shows good correlation with measurements performed in anechoic chamber at high frequencies [dB re 20 μ Pa/2.0 V at 1 m (1 W into 4 Ω)] and provides significant improvement at low frequencies. (b) Comparison of phase response.

ported loudspeaker system (20 Hz to 20 kHz) appears in Fig. 24.

Fig. 25 shows a comparison of the response of this ported loudspeaker measured using the simulated free field technique to the response of the same loudspeaker measured in an anechoic chamber. Here even greater differences can be observed at low frequencies than for the smaller closed-box system. The effects of inadequate low-frequency absorption in the chamber are more pronounced due to the use of a greater microphone distance for the far-field measurement, necessary because of a larger source size.

6 CHOICE OF TRANSITION FREQUENCY

Several possibilities exist for choosing the exact transition frequency f_s . In general, f_s should be chosen as high as possible in order to preserve low-frequency resolution, but above $1/T$. In any case it should be the near-field response that is manipulated relative to the far-field response. The level of the far-field response should not be altered, assuming it was calibrated. The first possibility would be to simply apply Eq. (24) and choose f_s

$= 1/T$. Choosing this transition frequency reduces the apparent resolution around f_s due to the "smoothing" effect of the time window on the measured far-field response at its lower frequencies, that is, in this frequency range there is more detail in the near-field measurement. Another method is to see if, after using Eq. (24), the two measurements intersect at some frequency. This frequency can then be used as f_s if it conforms to the aforementioned restrictions. Alternatively, the magnitude of the near-field response could be adjusted for a visual "best fit."

Because the drivers are generally mounted in an enclosure somewhat larger than the driver itself, at high frequencies (smaller wavelengths) the low-frequency drivers will no longer radiate spherically in the near field, due to the baffle effect of the enclosure [4], [7]. This effect is observed as a transition from 4π (spherical) to 2π (hemispherical) radiation, occurring over several octaves for increasing frequency, as the wavelength approaches the size of the source for sound radiation measured by a microphone placed in the near field. The useful upper frequency limit for near-field measurements on loudspeaker systems is always observed to be lower than the theoretical $f_{ka=1}$ limit for a driver mounted in

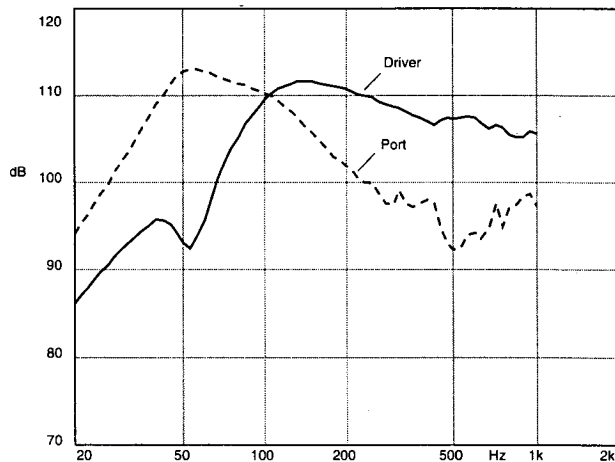


Fig. 22. Near-field measurements of driver and port performed on vented loudspeaker system (shown before scaling). Port response is scaled and then these complex responses are summed to obtain low-frequency response of system.

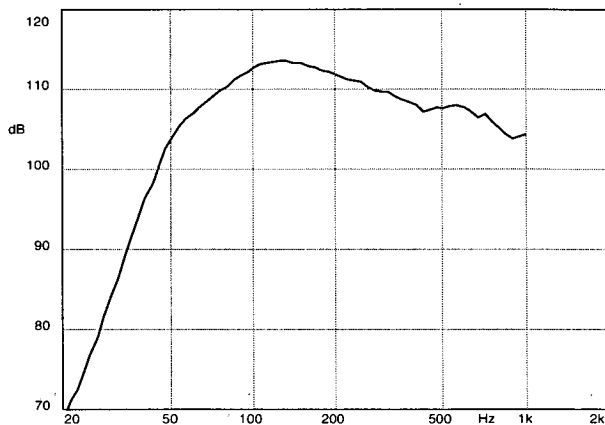


Fig. 23. Resulting near-field response of ported system. ($S_D = 127.68 \text{ cm}^2$, $S_P = 21.32 \text{ cm}^2$.)

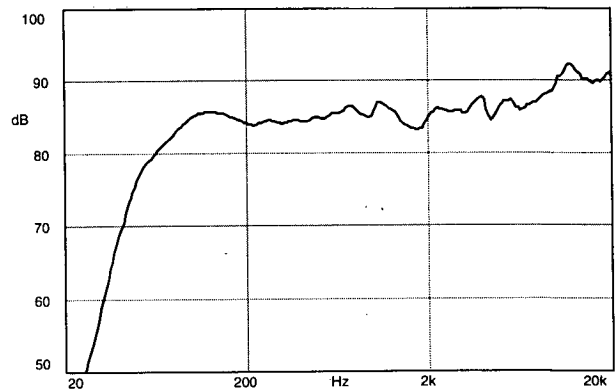


Fig. 24. Complete simulated free field frequency response of two-way 8- Ω ported loudspeaker, dB re 20 $\mu\text{Pa}/2.83 \text{ V}$ at 1 m (1 W into 8 Ω) measured on axis, grille off, $f_s = 206 \text{ Hz}$.

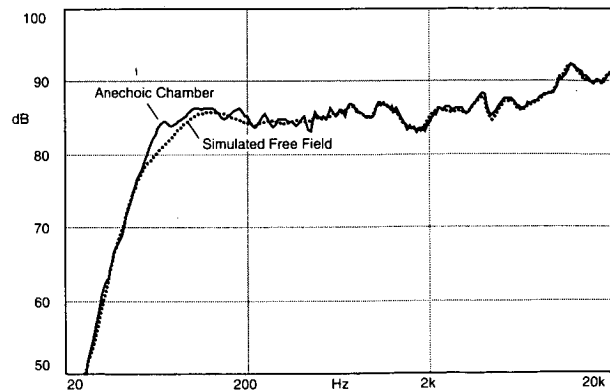


Fig. 25. Frequency response of ported loudspeaker measured using simulated free field technique and measured in anechoic chamber. Note irregularities in anechoic response caused by low-frequency reflections in anechoic chamber. Frequency response, dB re 20 $\mu\text{Pa}/2.83 \text{ V}$ at 1 m (1 W into 8 Ω).

a baffle. The near-field measurement will progressively under estimate the true free field response at higher frequencies. Because this limit is governed by the overall size of the test object, rather than by the driver radius, the entire enclosure must be considered when comparing the wavelength to the size of the source. In practice we have seen that the near-field response can be used with errors of less than 1 dB (Compared to anechoic measurements) at frequencies where the wavelength is greater than approximately 3 times the major dimension of the source M . An attempt to explain this behavior can be found by substituting M for $2a$ in Eq. (18). In terms of an upper limiting frequency, this is

$$f_s \leq \frac{c}{\pi M} \quad (29)$$

This is therefore the most critical factor governing the selection of f_s .

In practice the upper limit can also be verified by performing off-axis measurements to determine at what frequencies the source is no longer omnidirectional. For multiway systems with a crossover frequency f_x less than f_s , a lower transition frequency f_s should be chosen such that

$$f_s < f_x \quad (30)$$

to avoid rolloff in the near-field response due to the crossover filter.

7 HARMONIC DISTORTION

Using sinusoidal excitation also enables time-selective and near-field measurements of any selected harmonic components to be performed [5], [6]. Practical considerations for full audio bandwidth tests such as the range of human hearing, the frequency range of the measurement microphone, and the low energy level of upper harmonics outside the passband typically limit measurements to the second and third harmonics. More useful results for nonlinear measurements can be ob-

tained using two-tone techniques, but here the one-to-one relationship between time and frequency is lost and we are limited to measurements in an anechoic room or quasi-near-field measurements [10].

The measurement of a harmonic response results in a frequency multiplication of the desired response by the harmonic order for results plotted at the excitation frequency. Consequently the upper limiting frequency for near-field measurements is correspondingly reduced to the frequency where

$$ka = \frac{1}{N} \quad (31)$$

or

$$f_{ka=1} = \frac{c}{2\pi aN} \quad (32)$$

where N is the harmonic order. Fortunately the lower limiting frequency for far-field time-selective measurements is correspondingly lowered as well,

$$\Delta f = \frac{1}{NT} \quad (33)$$

Fig. 26 shows the separation of individual harmonic components in time and frequency for a linearly swept sinusoidal excitation. Each far-field harmonic must therefore be measured with an individual sweep in order to isolate the desired component from reflections and other harmonics. The near-field harmonics can be tested at discrete frequencies in a single pass. The transition frequency for each harmonic, $f_s(N)$, should also be a function of the harmonic order,

$$f_s(N) = \frac{f_s(1)}{N} \quad (34)$$

where $f_s(1)$ is the transition frequency selected for the fundamental.

Harmonic distortion measurements were performed on

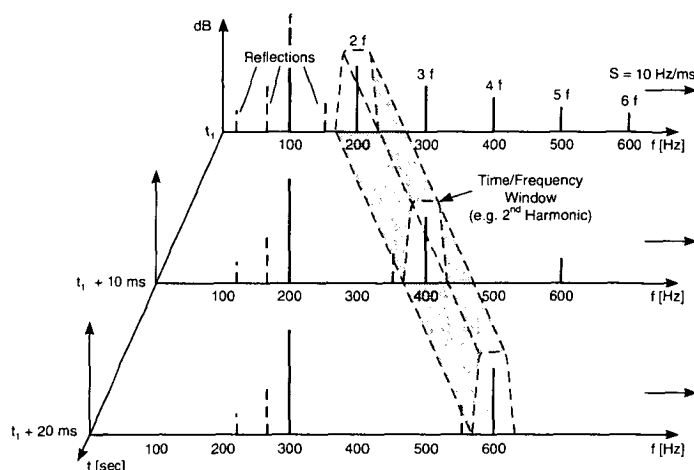


Fig. 26. Use of linearly swept sinusoidal excitation signal enables time-selective measurements of individual harmonic components to be performed. Diagram shows separation of second harmonic in time and frequency.

the closed-box loudspeaker using this technique (see Fig. 27). Note that these are true harmonic responses (not THD plus noise). The total harmonic distortion (THD) referred to the total is calculated as

$$THD = \frac{\sqrt{H_2(f)^2 + H_3(f)^2}}{\sqrt{H_1(f)^2 + H_2(f)^2 + H_3(f)^2}} \quad (35)$$

where the denominator (total) is the power sum of the fundamental plus the measured harmonics (in this case, the second and third). The resulting THD compared to the total is shown in Fig. 28. Good correlation was found with equivalent measurements performed in an anechoic chamber, especially at higher frequencies (see Fig. 29).

8 CONCLUSION

A technique has been presented enabling measurements of the complex free field response of a loudspeaker to be performed, without an anechoic room, throughout the entire audio frequency range. One measurement is performed using a time-selective technique in the far field of the source. The low-frequency response is then obtained using the near-field technique. Assuming an overlap frequency range exists, a transition frequency can be selected at which to join these measurements.

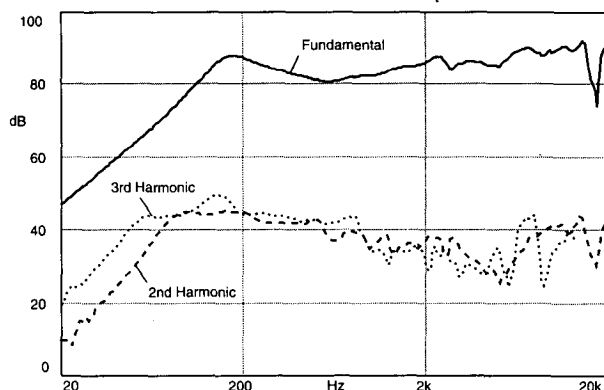


Fig. 27. Fundamental, second, and third harmonic responses of closed-box loudspeaker for 2.83-V input, measured using simulated free field technique. Responses are in dB SPL re 20 μ Pa referred to 1 m.

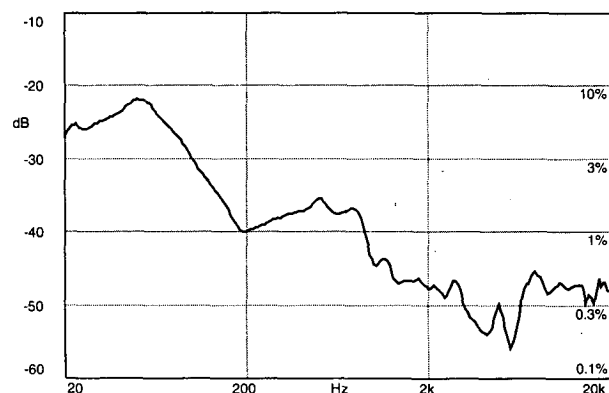


Fig. 28. Resulting total harmonic distortion in dB re total and in %.

The sine-based test methods employed to test technique optimize speed and the selectivity in both time and frequency, and maximize the available signal-to-noise ratio. In addition, sinusoidal excitation provides a low crest factor signal and enables accurate specification of the input power to the device under test. This technique also presents the resulting data optimally in both the frequency and the time domains. These results are available in any desired coordinates and can be exported for further processing. Furthermore it has been demonstrated that, using sine-based analysis, this technique can be extended to include measurements of harmonic distortion. The only limits for this technique are, in fact, imposed by the size of the room used for performing the tests. These limits, however, are much less critical than with either purely time-selective techniques alone or traditional measurements in an anechoic chamber. The effects of the anechoic chamber on the measured response at low frequencies, caused by its limited size and insufficient absorption of low-frequency reflections, are eliminated. A comparison to traditional anechoic measurements clearly reveals the magnitude of these chamber-induced errors. This technique offers reliability and convenience without making unnecessary assumptions about the environment or about the device under test.

9 ACKNOWLEDGMENT

The authors wish to thank Thomas V. Petersen for his help in preparing the manuscript.

10 REFERENCES

- [1] C. H. Biering and O. Z. Pedersen, "Free Field Techniques—A Comparison," Brüel & Kjær (1981).
- [2] R. Heyser, "Acoustical Measurements by Time Delay Spectrometry," *J. Audio Eng. Soc.*, vol. 15, p. 370 (1967 Oct.).
- [3] C. H. Biering and O. Z. Pedersen, "System Analysis and Time Delay Spectrometry, Part 1," *Brüel & Kjær Tech. Rev.*, no. 1 (1983).
- [4] L. R. Fincham, "Refinements in the Impulse Test-

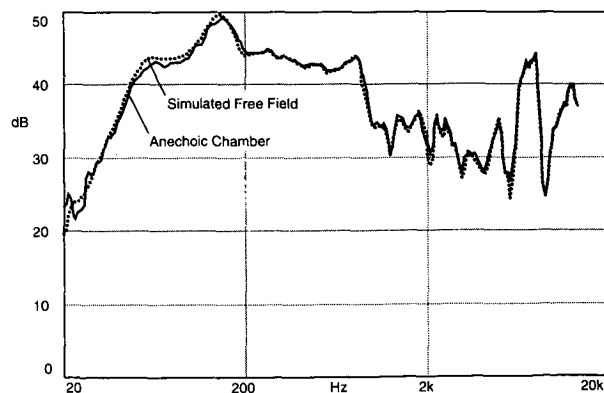


Fig. 29. Comparison between third-harmonic measurements performed using simulated free field technique and measurements performed in anechoic chamber. Frequency response, dB re 20 μ Pa/2.83 V at 1 m (1 W into 8 Ω).

ing of Loudspeakers," *J. Audio Eng. Soc.*, vol. 33, pp. 133–140 (1985 Mar.).

[5] C. J. Struck and C. H. Biering, "A New Technique for Fast Response Measurements Using Linear Swept Sine Excitation," presented at the 90th Convention of the Audio Engineering Society, *J. Audio Eng. Soc. (Abstracts)*, vol. 39, p. 384 (1991 May), preprint 3038.

[6] C. J. Struck, "An Adaptive Scan Algorithm for Fast and Accurate Response Measurements," presented at the 91st Convention of the Audio Engineering Society, *J. Audio Eng. Soc. (Abstracts)*, vol. 39, p. 1004 (1991 Dec.), preprint 3171.

[7] D. B. Keele, Jr., "Low-Frequency Loudspeaker Assessment by Nearfield Sound-Pressure Measurement," *J. Audio Eng. Soc.*, vol. 22, pp. 154–162 (1974 Apr.).

[8] L. L. Beranek, *Acoustics* (American Institute of Physics for the Acoustical Society of America, Cambridge, MA, 1986).

[9] J. Vanderkooy and S. P. Lipshitz, "Uses and Abuses of the Energy-Time Curve," *J. Audio Eng. Soc.*, vol. 38, pp. 819–836 (1990 Nov.).

[10] S. F. Temme, "Why and How to Measure Distortion in Electroacoustic Transducers," *Proc. AES 11th Int. Conf. on Audio Test and Measurement*, Portland, OR, 1992 (May 29–31).

APPENDIX 1 dB REFERENCE

The magnitude of the frequency response of a loudspeaker is usually plotted in decibels versus frequency. In order to be able to interpret this curve correctly, it is necessary to know the decibel reference. Recall that decibels express a logarithmic power ratio,

$$\text{dB} = 10 \log_{10} \frac{P}{P_0} \quad (36)$$

where P_0 is the reference power.

Normally power is not measured directly. Therefore this expression can be rewritten as

$$\text{dB} = 20 \log_{10} \frac{x}{x_0} \quad (37)$$

where x_0 is the corresponding signal reference. This is derived from the fact that the ratio of the squares of two signals is equal to the ratio of their powers. The reference for a transfer function has dimensions and can be found by dividing the reference for the output by the reference for the input. For a loudspeaker x_0 is in pascals per volt. Therefore if the output is desired in dB SPL, the output reference is 20 μPa .

Typically the reference for the input is given as a power (such as 1 W). The signal applied, however, is in volts, so the power will depend on the impedance of the loudspeaker. In general the voltage is found that will dissipate the reference power across a resistance equal

to the loudspeaker's specified nominal impedance,

$$P_0 = \frac{V^2}{Z_0} \quad [\text{W}] \quad (38)$$

so

$$V = \sqrt{P_0 Z_0} \quad [\text{V}] \quad (39)$$

where V is the corresponding input reference voltage. This refers the measured response to the reference power, regardless of the actual level of the excitation signal. This of course assumes that the device under test behaves linearly (that is, no power compression).

Because the output terminals of a loudspeaker are not intrinsically obvious, it is also necessary to specify a reference distance. Typically this is 1 m. For free field measurements of a point source (that is, spherical sound radiation), the sound pressure level is inversely proportional to the distance (a -6-dB change in output level for every doubling of distance). This is easily verified empirically. As explained earlier, it may be necessary to perform measurements at some distance other than the reference distance in order to be in the far field of the source. Fortunately this can easily be incorporated into the dB reference using either distance or time delay, assuming a constant speed of sound. The complete reference then becomes

$$x_0 = \frac{P_0}{\sqrt{P_0 Z_0}} \cdot \frac{d_0}{d} \quad [\text{Pa/V}] \quad (40)$$

Typically p_0 is 20 μPa , P_0 is 1 W, and d_0 is 1 m. For example, for an $8\text{-}\Omega$ loudspeaker measured at 1 m ($Z_0 = 8\ \Omega$ and $d = 1\text{ m}$), $x_0 = 7.07\ \mu\text{Pa/V}$.

For a constant speed of sound c time delay can be equated to distance as

$$\tau = \frac{d}{c} \quad [\text{s}] \quad (41)$$

In terms of time delay, the dB reference can then be written as

$$x_0 = \frac{P_0}{\sqrt{P_0 Z_0}} \cdot \frac{\tau_0}{\tau} \quad [\text{Pa/V}] \quad (42)$$

For $c = 344\ \text{m/s}$ and $d_0 = 1\ \text{m}$, $\tau_0 = 2.91\ \text{ms}$. Normally the time delay can be obtained directly from the magnitude of the time response by locating the largest peak, corresponding to the arrival of the direct sound.

For line sources, such as tall, narrow ribbon loudspeakers and tweeter line arrays, the sound pressure level changes by $-3\ \text{dB}$ for every doubling of distance of the measurement microphone under free field conditions (recall Fig. 4). Applying this relationship, the dB reference becomes

$$x_0 = \frac{P_0}{\sqrt{P_0 Z_0}} \cdot \sqrt{\frac{d_0}{d}} \quad [\text{Pa/V}] \quad (43)$$

or, in terms of time delay,

$$x_0 = \frac{P_0}{\sqrt{P_0 Z_0}} \cdot \sqrt{\frac{\tau_0}{\tau}} \quad [\text{Pa/V}] \quad (44)$$

This is also easily verified empirically. Of course, if d is increased sufficiently, even a line source will appear to behave like a point source. Provided the measurements are calibrated, the loudspeaker sensitivity and directivity can easily be calculated from these dB values.

APPENDIX 2 NEAR-FIELD MEASUREMENTS OF PORTED ENCLOSURES AND MULTIPLE-DRIVER SOURCES

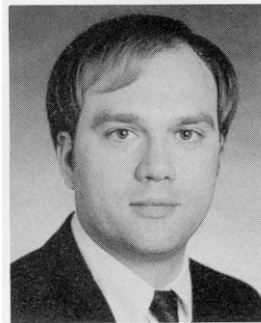
The low-frequency response of ported loudspeakers and loudspeakers containing multiple drivers can also

be measured using the near-field technique described by Keele [7]. The complex response of each source (driver or port) should be measured individually. These complex responses can then be summed. The overall near-field response is given by

$$H_{\text{NF}}(f) = H_{\text{D}}(f) + \sqrt{\frac{S_{\text{P}}}{S_{\text{D}}}} H_{\text{P}}(f) \quad (45)$$

where $H_{\text{D}}(f)$ is the near-field measurement of the driver, S_{P} is the total radiating surface area of the port(s), S_{D} is the total radiating surface area of the driver(s), and $H_{\text{P}}(f)$ is the near-field measurement of the port. When measuring the port response, the microphone should be positioned in the same plane as the port opening (see Fig. 8). Passive-radiator systems can also be measured with this method. In this case the passive elements are simply treated as ports.

THE AUTHORS

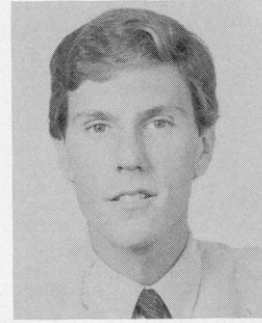


C. J. Struck

Christopher J. Struck was born in Milwaukee, WI, in 1962. He is a graduate of the Electrical Engineering School of the University of Wisconsin-Madison. From 1983 to 1985, he worked in the UW Electroacoustics Lab, developing circuitry for transducer measurements, sound intensity research, and active noise control applications. During this time, he also studied electronic music composition and *musique concrète*, producing multimedia concerts and works for modern dance. In 1985, Mr. Struck attended Stanford University, where he studied digital signal processing and participated in the Stanford Jazz Workshop.

In 1986, he joined Brüel & Kjær. From 1988 through 1993, he lived in Denmark, working as an application specialist in electroacoustics. There, he helped to develop new measurement techniques and new instrumentation for testing electroacoustic transducers, most notably the Type 4128 head and torso simulator and the Type 2012 audio analyzer. During the course of his work, he has traveled extensively throughout the world providing training and lecturing on the topics of electroacoustics, telephonometry, linear and nonlinear system analysis, and measurement techniques. Currently, he is a principal consultant with Charles M. Salter Associates in San Francisco, California.

Mr. Struck is the author of many technical papers, application notes and articles, several of these coauthored with his friend and colleague Steve Temme. He is a member of the Audio Engineering Society, the Institute of Electrical and Electronics Engineers, and the



S. F. Temme

Acoustical Society of America. He is on the IEEE Subcommittee on Telephone Instrument Testing and the AES SC-4-3 Working Group on Loudspeaker Modeling and Measurement. He is a guitarist and composer and enjoys both live and recorded music. Mr. Struck lives in San Francisco.

Steve Temme was born in Boston, MA, in 1962. From 1980 to 1985, he attended Tufts University, majoring in mechanical engineering. During this time, he also ran a successful business selling stereo equipment, which helped finance his education. He received the B.S.M.E. from Tufts in 1985.

He was first employed by Brüel & Kjær Instruments in Marlborough, MA, in October of 1985 as a sales engineer for the northeastern region of the United States. In 1988, Mr. Temme joined Apogee Acoustics in Randolph, MA, as a loudspeaker design engineer. There, he worked on the development of the Stage full-range, dipole, ribbon loudspeaker and on the DAX active crossover system. In 1990 he moved to Denmark where he was employed by Brüel & Kjær as an audio application specialist. There, he worked with the Type 2012 audio analyzer, training engineers, giving seminars, and developing loudspeaker and microphone measurement programs.

Mr. Temme currently works as an independent consultant in audio and electroacoustics in Boston. He is a member of the AES and an avid concert-goer and hi-fi enthusiast.